



Mechanical and Durability Performance of Fly Ash on Bauxite Residue and Ground Granulated Blast Slag Based Geopolymer Composite

Bheem Pratap¹ · Pooja Kumari² · B. Hanumantha Rao³ · Somenath Mondal¹

Received: 22 September 2023 / Accepted: 22 March 2024 / Published online: 18 April 2024
© The Author(s), under exclusive licence to Shiraz University 2024

Abstract

This study looked at the utilization of industrial by-products to create a workable geopolymer concrete (GPC) for construction work. The industrial by-products used in this study are bauxite residue (BR), fly ash (FA), and ground granulated blast slag (GGBS). Geopolymerization involves utilizing these industrial by-products as the basis for creating GPC, a sustainable and long-lasting alternative to conventional cement. In this study, BR was replaced with FA and GGBS. The mechanical and durability properties of the geopolymer concrete were analyzed. The maximum compressive strength obtained was 65.56 MPa for RFG5 specimen, which can be used in construction applications. The specimens RFG5 shows the minimum water absorption, porosity, charge passed and mass loss to different environmental conditions. The gel formation of the GPC can be observed from the energy dispersion spectroscopic images and X-ray diffraction (XRD) to increase the strength of GPC. However, the problem faced in this study was developed during the preparation of the alkali solution and curing of the specimens.

Keywords Industrial byproducts · Compressive strength · RCPT · XRD · Leaching

1 Introduction

Industrial by-products, often considered waste products, can be transformed into valuable resources through the development of geopolymerization. Geopolymerization is a technique that utilizes these by-products as a raw material to produce geopolymer, a durable and environmentally friendly alternative to traditional cement. This innovative approach not only addresses the issue of waste disposal but also offers

numerous benefits in various applications. Bauxite residue, also known as red mud, is a by-products generated during the extraction of alumina from bauxite ore in the Bayer process (Mishra et al. 2020). It is primarily composed of iron oxide, silicon dioxide, titanium dioxide, and other minor elements (Alam et al. 2019). Traditionally, bauxite residue has been considered a waste material and stored in large containment areas, which can pose environmental challenges. However, in recent years, there has been growing interest in utilizing bauxite residue as a valuable resource in various applications, including geopolymer production (Pratap et al. 2023c). Bauxite residue presents an attractive source of aluminosilicate material for geopolymer production, offering a sustainable solution for utilizing this abundant waste material (Pratap et al. 2023a). The basic uses of bauxite residue in geopolymer applications is in the production of construction materials (Zhang et al. 2021). By substituting bauxite residue for traditional raw materials, such as FA or GGBS, in the geopolymer synthesis process, it is possible to create binder materials that exhibit excellent strength and durability. Another potential use of bauxite residue in geopolymer technology is in the immobilization of hazardous (Sarath Chandra and Krishnaiah 2022). Geopolymer matrices can effectively encapsulate and immobilize toxic contaminants

✉ Somenath Mondal
smondal.ce@nitjsr.ac.in

Bheem Pratap
2018rsce007@nitjsr.ac.in

Pooja Kumari
2021rsee005@nitjsr.ac.in

B. Hanumantha Rao
bhrao@iitbbs.ac.in

¹ Department of Civil Engineering, National Institute of Technology Jamshedpur, Jharkhand 831014, India

² Department of Electrical Engineering, National Institute of Technology Jamshedpur, Jharkhand 831014, India

³ School of Infrastructure, Indian Institute of Technology Bhubaneswar, Odisha 752050, India

due to their excellent chemical resistance and long-term stability. By incorporating bauxite residue into the geopolymer matrix, it is possible to enhance its ability to immobilize heavy metals and other pollutants (Toniolo et al. 2018). This application has significant environmental implications, as it can help remediate contaminated sites and prevent the leaching of harmful substances into the surrounding environment (Jatoliya et al. 2023). Bauxite residue can serve as a valuable precursor for the synthesis of geopolymer ceramics, enabling the development of advanced materials with enhanced performance characteristics (Kumar and Kumar 2013; Liang and Ji 2021; Muraleedharan and Nadir 2021a; Sudhir et al. 2020; Zhou et al. 2020).

FA is a fine powder produced from coal combustion in power plants. Traditionally, fly ash has been disposed of in landfills, posing environmental challenges (Koshy et al. 2019; Liu et al. 2016; Ngarm et al. 2015; Tammam et al. 2021; Xie and Ozbakkaloglu 2015). However, by converting fly ash into a geopolymer, its utilization potential is maximized. Geopolymer not only reduces the environmental impact of fly ash disposal but also presents several advantageous properties.

A byproduct known as GGBS is generated in the blast furnace when iron is manufactured (Deb et al. 2014; Nath and Sarker 2017). Because GGBS has good pozzolanic qualities, it has been exploited as a supplemental resource (Liang and Ji 2021). Enhancing the mixture's workability is a noteworthy advantage of employing GGBS in geopolymer (Alam et al. 2019). The geopolymer mixture is simpler to pour and put because GGBS increases flow and reduces viscosity. Enhancing GPC's strength and durability is one of the main applications of GGBS in geopolymer (Singh et al. 2018). When combined with calcium hydroxide, GGBS is a great pozzolanic that produces calcium alumino-silicate hydrate gel (C-A-S-H), which increases the durability and strength of geopolymer concrete (Shahmansouri et al. 2021; Zhang et al. 2020a).

The maximum compressive strength of 59 MPa was obtained of fly ash based geopolymer concrete (Naenudon et al. 2023). The possible application of fly ash in the production of geopolymer was identified by Koshy et al. (2019) who also found that the FA was included into BR to increase the geopolymer's efficacy (Koshy et al. 2019). Hoang et al. (2020) investigation into BR as a precursor material for alkali activation looked at the process of combining BR with FA and discovered that the addition of active silica increased compressive strength by 20 MPa when 26.3 weight percent of BR was replaced with FA (Hoang et al. 2020). A prospective research on BR-FA for the production of geopolymer was carried out by Yang et al. (2019) and they found that a ratio of 1:4 was ideal. It may be possible to use the enormous quantity of PG waste in the building industry by combining fly ash with BR (Yang et al. 2019).

Moreover, geopolymerization can utilize other industrial byproducts such as slag from the iron and steel industry. By incorporating slag into geopolymer, its harmful environmental impact can be mitigated while creating a valuable construction material (John et al. 2021; Liang and Ji 2021; Ma et al. 2022; Ren et al. 2023; Vafaei et al. 2021). Geopolymer materials exhibit excellent mechanical strength, chemical resistance, and durability. One of the most significant uses of geopolymer is in construction. Geopolymer concrete shows excellent resistance to corrosion, and chemical attacks, making it a highly desirable material for infrastructure projects (Chen et al. 2021; Li et al. 2021; Muraleedharan and Nadir 2021b).

The mechanical and durability study of fly ash, GGBS, and BR has been analyzed in previous literature. However there is a research gap, researchers have typically focused on studying one or two industrial by-products. In this study, mechanical and durability analyses were performed by combining these three by-products. The objective of this study is to develop GPC by incorporating BR, FA, and GGBS, and evaluate its mechanical and durability properties for potential use as construction materials for pavement and building. The BR was replaced with FA at fixed GGBS content with 5, 10, 15, 20, 25, 30 and 35%. The novelty of this research involves examining the compressive strength, flexural strength, and split tensile strength of the developed GPC from industrial by-products BR, FA and GGBS. Additionally, the study investigates the GPC's performance in rapid chloride penetration test (RCPT), water absorption and porosity tests. The aggressive environment studies were also conducted in acid, chloride and sulfate solution. Microcharacterization of the GPC is carried out using energy dispersion spectroscopic (EDS) and XRD analysis of the specimens after 28 days curing periods. Toxicity characteristics of leaching potentials is also study to analyse the leaching of the heavy metal concentration.

2 Materials and Methods

The materials used in this study were sourced from different locations. BR, fly ash and GGBS were collected from Muri, Usha Martin and TATA steel plant respectively in Jharkhand. The specific gravity of BR, FA, and GGBS were determined to be 3.16, 2.83, and 2.94, respectively. The NaOH and Na₂SiO₃ used in this study were purchased from local supplier of 98% purity. The coarse aggregate and fine aggregate used in this was also taken from local supplier. The oxides composition of the BR, FA and GGBS is given in Table 1.

Table 1 Major oxides composition of the materials

Oxides compositions	BR	FA	GGBS
SiO ₂	17.32	58.43	30.24
Fe ₂ O ₃	36.45	17.52	10.45
Al ₂ O ₃	16.36	25.45	14.61
CaO	2.18	2.62	33.38
Na ₂ O	14.71	0.56	0.78
TiO ₂	8.11	1.17	0.84
K ₂ O	0.37	0.48	0.52
SO ₃	0.19	0.17	1.57
P ₂ O ₅	0.43	0.57	–

2.1 Mix Procedure

Table 2 illustrates the substitution of different proportions of FA and GGBS for BR. The alkali solution was prepared with distilled water. To establish the optimum alkali solution to binder ratio, several tests were performed, and the ideal ratio was determined to be 0.4. The Na₂SiO₃ to NaOH ratio keep constant at 1.5 in all specimens at constant 12 M NaOH. The dry mixing of BR, FA, GGBS, CA, and fine aggregate were mixed for 5 min, followed by an additional 4 min of mixing with the alkali solution. After casting, all specimens were cured at 70 °C for 24 h, subjected to temperature of 27 °C curing for 28 days.

2.2 Tests

2.2.1 Mechanical Properties

Slump tests were performed to assess the workability after mixing (ASTM C143/C143M—10 2014). IS:10,086 (2004) specifies the criteria for moulds utilized in the casting of concrete cubes, cylinders, and beams, designed for conducting tests on concrete materials. Series of strength tests conducted on different types of concrete samples as per the IS:10,086 (2004) standard. Cube-shaped samples with

size of 150 mm × 150 mm × 150 mm are cast and cured for specific periods (3, 7, and 28 days). Prism-shaped specimens with size of 100 mm × 100 mm × 500 mm are cast and cured for the same durations as the compressive strength test. Cylindrical samples with a diameter of 150 mm and a height of 300 mm are cast and cured (IS:10,086 2004). In each of these tests, three specimens are tested and the average of the results is reported. The tests are carried out at different curing periods (3, 7, and 28 days) to assess how the strength of the concrete develops over time. The experimental work of the mixing and casting of the specimens have been shown in Fig. 1.

2.2.2 Durability Test

The rapid chloride penetration test (RCPT) is a test method specified by ASTM C1202 2012 to assess the resistance of concrete against chloride ion penetration (Fig. 2) (ASTM C1202 2012). The long-term performance of concrete infrastructure is predicted by this test, which is essential to preserving its durability (Fernando et al. 2023). This test was conducted on AAC specimens that were 50 mm thick and 100 mm in diameter (Sahu et al. 2024). Figure 2 depicts the RCPT testing protocol and sample set. Every thirty minutes for duration of six hours, the current (I) pass was documented (Pratap et al. 2024). On the other hand, ASTM C642 2013 is followed to evaluate the porosity and water absorption characteristics of GPC samples (ASTM C642 2013). On the other hand the aggressive environmental effect was performed in acid, chloride and sulfate solution. The chemical used for the acid, chloride and sulfate tests were H₂SO₄, NaCl and MgSO₄ respectively. The concentration of the aggressive environmental solution were 5, 2 and 3% taken for chloride, acid and sulfate solution respectively for 60 days. The GPC specimens of the same mix were cured in normal water for the comparative analysis of the specimens. The test is performed on cured specimens of GPC after 28 days.

Table 2 Mix design of GPC

Mix ID	BR (Kg/m ³)	FA (Kg/m ³)	GGBS (Kg/m ³)	Coarse aggregate (CA) (Kg/m ³)	Fine aggregate (Kg/m ³)	NaOH (Kg/m ³)	Na ₂ SiO ₃ (Kg/m ³)
RFG1	374	22	44	1150	640	72	108
RFG2	352	44	44	1150	640	72	108
RFG3	330	66	44	1150	640	72	108
RFG4	308	88	44	1150	640	72	108
RFG5	286	110	44	1150	640	72	108
RFG6	264	132	44	1150	640	72	108
RFG7	242	154	44	1150	640	72	108



Fig. 1 Photograph of experimental work during mixing and casting of specimens

Fig. 2 RCPT test set up with specimens



2.2.3 Toxicity Characteristics of Leaching Procedure

The Toxicity Characteristics Leaching Procedure (TCLP) is a standardized method used to determine the potential for hazardous waste to leach toxic contaminants into the environment (Alam et al. 2019). The TCLP test assesses the mobility of specific heavy metals present in the waste, providing valuable information to ensure proper waste management and protect human health and the environment (Ren et al. 2023). The TCLP test was developed by the United States Environmental Protection Agency (EPA) and is now widely adopted and recognized internationally (EPA 1996). The test is conducted on a representative sample of the waste material using an acidic leaching solution that simulates the conditions found in specimens (Apithanyasai et al. 2020). The sample is dried and sieved to remove coarse particles. It is then mixed with an acidic leaching solution that mimics the pH. The mixture is agitated for 18 h. During the leaching process, heavy metals and organic compounds present in the waste can dissolve

into the leachate solution (Mishra et al. 2020). The leachate is then analyzed to determine the concentration of specific toxic contaminants. The photograph of the experiment has been shown in Fig. 3.

3 Results and Discussions

3.1 Fresh Properties

Workability is the simplicity with which a freshly mixed concrete may be handled, placed, compacted, and finished. Concrete's workability is often evaluated using the slump test. The standard slump test in accordance with ASTM C 143 was used to measure the workability of fresh geopolymer concrete shortly after the concrete had been mixed. According to Fig. 4, the slump rises first, then falls, and reaches a maximum of 97 mm at 25% FA concentration. The morphological impact of FA is one factor. The majority of FA particles have spherical shapes and



Fig. 3 TCLP test set up with specimens

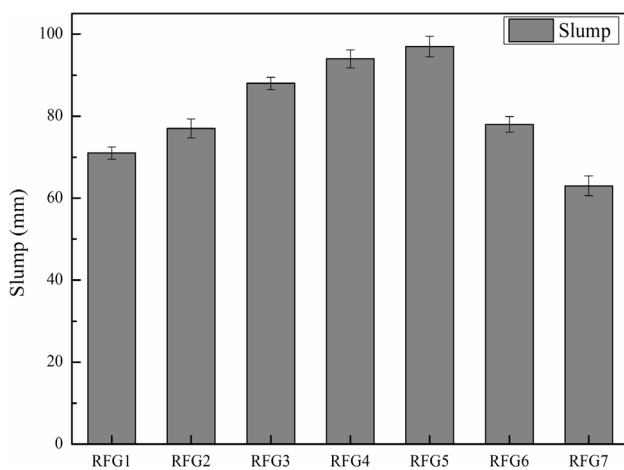


Fig. 4 Slump variation of geopolymer concrete

smooth surfaces. FA added to GPC functions like a ball bearing, lubricating the particles of uneven material (Yin et al. 2022). The fineness of FA is also more superior than that of BR and GGBS. It is conjectured that the operating performance of the GPC would vary depending on the FA's fineness. Less alkali is needed as FA particle size and spherical particle concentration increase (Fareed Ahmed et al. 2011). At 5% FA concentration, the slump measured 71 mm, which is 28 mm less than at 25% FA level. A correct FA concentration will enhance GPC density, which will cause the alkali solution to discharge into the pores and produce a thicker film. The alkali film thins and the slump lessens as the FA concentration exceeds the crucial amount of 25%. In other words, FA as a fine aggregate can simultaneously increase the strength and fluidity of the backfilled sample within a limited dose range (Li et al.

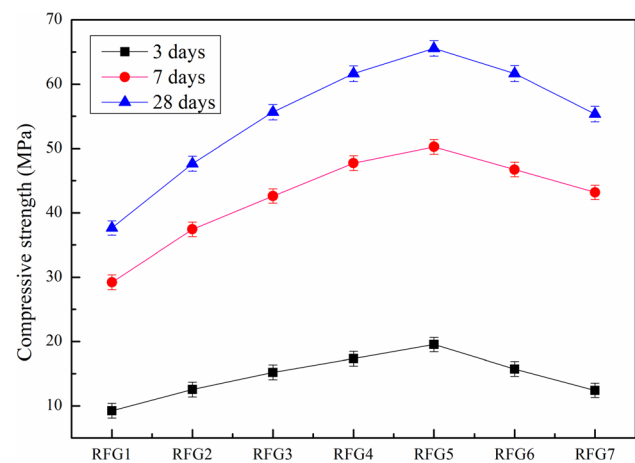


Fig. 5 Compressive strength variation with days

2020). This state is mostly attributable to the usage of FA as a fine aggregate to fill the waste skeleton rather than to reduce the need for BR and GGBS. The inclusion of FA improves the material's compactness while also promoting the growth of strength.

3.2 Compressive Strength

Figure 5 presents the compressive strength results of GPC at different curing periods. The graph shows that the compressive strength of all the geopolymer samples increases over time and with the adding of fly ash. This growth in strength can be endorsed to the production of geopolymerization process (Lian et al. 2023; Pratap et al. 2023c; Sun et al. 2022; Tanyildizi and Yonar 2016; Zakira et al. 2023). The compressive strength values of geopolymer samples at 3, 7, and 28 days after casting have been provided (Fig. 5).

At 3 days, the compressive strength values range from 9.24 to 19.53 MPa for different samples (RFG1, RFG2, RFG3, RFG4, RFG5, RFG6 and RFG7). These values demonstrate the initial strength of the geopolymer concrete and show that it increases with the addition of fly ash. Fly ash, being a pozzolanic material, contributes to the geopolymerization process, resulting in improved early-age strength (Durak et al. 2021). Moving on to the 7-day results, the compressive strength values have significantly increased compared to the 3-day results. The values range from 29.21 MPa to 50.26 MPa for the same samples. This substantial strength gain over the 7-day curing period indicates the progression of the geopolymerization process and the continued development of the binding matrix (Iqbal et al. 2023). As the reaction between the aluminosilicate materials and the alkaline activator continues, the geopolymer concrete gains more strength. Finally, at 28 days, the compressive strength values reach their peak values, ranging from 37.64 to 65.56 MPa for the respective samples. As per IRC 58 (2011) the minimum compressive strength of the concrete is 40 MPa (IRC 58 2011 2011). Hence based on the results the developed composite materials can be used in rigid pavement application. These values represent the ultimate strength attained by the geopolymer concrete after the full curing period. The mix RFG5 resulted maximum compressive strength. These values represent the ultimate strength attained by the geopolymer concrete after the curing period (Bellum et al. 2020a). The results demonstrate a continuous increase in strength, reflecting the progressive development of the GPC.

When examining the impact of fly ash content on the compressive strength of bauxite residue mixed with a constant 10% GGBS, some interesting trends can be observed. Initially, as the FA content increases from 5 to 25%, the compressive strength of the mixture shows an improvement (Fig. 5). This can be attributed to the beneficial properties of fly ash, such as its pozzolanic nature, which allows it to react with calcium hydroxide in the presence of water, resulting in the formation of additional geopolymer compounds (Bellum et al. 2020b; Chen and Yuan 2022; Kuri et al. 2021; Meskini et al. 2022). These compounds contribute to the overall strength development of the mixture. However, beyond a fly ash content of 25%, a different trend emerges. The compressive strength starts to decrease as the FA content increases further (Fig. 5). The excess FA particles may start to interfere with the packing and interlocking of the particles in the mixture, leading to a less compact structure (Badkul et al. 2021). This can result in reduced strength. It is worth noting that the specific percentages mentioned (5%, 25%, and beyond) may vary depending on the specific composition of the bauxite residue and GGBS used, as well as other factors such as curing conditions and testing methods (Pratap et al. 2023d). Therefore, 25% is the optimum fly ash content for achieving the desired compressive strength.

3.3 Flexural Strength

Figure 6 presents the flexural strength results of GPC samples at different ages. The data shows that the flexural strength of all GPC samples follows a similar pattern to the compressive strength. At the initial curing period of 3 days, the flexural strength values for seven GPC samples, namely RFG1, RFG2, RFG3, RFG4, RFG5, RFG6, and RFG7, were measured and recorded. These values ranged from 1.86 to 2.91 MPa. It is observed that as the curing period progresses to 7 days, there is a significant increase in the flexural strength for all samples. The flexural strength values at 7 days were between 4.42 to 6.85 MPa, representing a notable improvement over the initial curing period. Continuing through the curing period to 28 days, the flexural strength of the GPC samples continued to improve. The flexural strength values at 28 days ranged from 6.14 to 9.35 MPa, representing a notable improvement over the initial curing period. Continuing through the curing period to 28 days, the flexural strength of the GPC samples continued to improve. The flexural strength values at 28 days ranged from 6.14 to 9.35 MPa. As per IRC 58 (2011) the minimum flexural strength of the concrete is 5 MPa (IRC 58 2011 2011). Hence based on the results the developed composite materials can be used in rigid pavement application. This trend indicates that the curing process plays a crucial role in enhancing the mechanical properties of the GPC samples, making them more resilient and suitable for pavement application. It is important to note that these GPC mixes differ in the composition and proportions of materials used, specifically BR, FA, and GGBS. The uppermost flexural strength of 9.35 MPa at 28 days was achieved when bauxite residue was substituted with 25% FA and 10% GGBS, as seen in the RFG5 sample. This indicates that the insertion of FA in the GPC mix enriched the strength.

The observed rise in flexural strength with curing time can be attributed to the growth of the geopolymer matrix (Sarath Chandra and Krishnaiah 2022). Geopolymerization is a chemical process that occurs when alkali activators, such as sodium hydroxide and sodium silicate, react with source

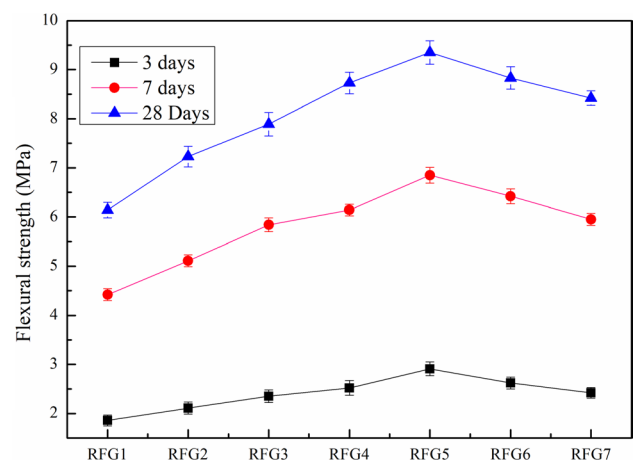


Fig. 6 Flexural strength variation with days and mix ID

materials with BR, FA, and GGBS. As the geopolymerization reaction progresses, the binder matrix undergoes further hardening and gains strength. The incorporation of FA in the GPC mix positively influenced the flexural strength. Fly ash is known to contain reactive components that contribute to the geopolymerization process. These reactive components, such as silica and alumina, react with the alkali activators, forming a geopolymer gel that enhances the binding properties and overall strength of the specimen (Adamu et al. 2022; Ryu et al. 2013; Shi et al. 2022).

3.4 Split Tensile Strength

Figure 7 displays the split tensile strength of GPC. The results indicate that the split tensile strength of all GPC developed using different combinations of BR, FA, and GGBS follows a similar pattern as the compressive and flexural strength. This suggests that the factors influencing the development of split tensile strength are similar to those affecting compressive and flexural strength. At 3 days of curing, the split tensile strength values are relatively low for all GPC mixes, ranging from 1.15 to 2.86 MPa. This initial strength is typical for young concrete, and it is still gaining strength as the hydration process progresses. As the curing period extends to 7 days, there is a notable increase in split tensile strength for all GPC mixes. The values now range from 2.42 to 3.85 MPa, showcasing a considerable improvement compared to the 3-day strength values (Fig. 7). This surge is attributed to the continued hydration of cementitious materials, resulting in increased bonding and interlocking of concrete particles (Özkılıç et al. 2023). After 28 days of curing, the split tensile strength values see another significant rise. Now, the strengths range from 3.76 to 6.12 MPa (Fig. 7). The 28-day mark is often considered a benchmark for concrete strength as it signifies the majority of the hydration

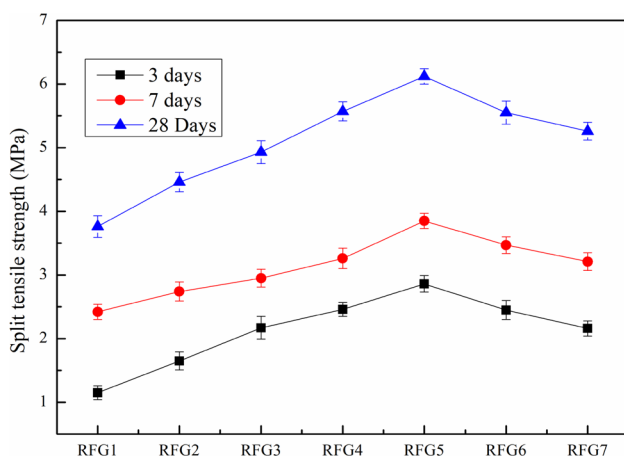


Fig. 7 Split tensile strength variation with days and mix ID

process is complete. The prolonged curing period allows for more complete cement hydration, leading to a denser and stronger concrete matrix (Meesala et al. 2020). Among the tested GPC mixes, RFG5 exhibits the highest split tensile strength of 6.12 MPa after 28 days (Fig. 7). This result indicates that the specific combination of materials used in RFG5 resulted in the most favorable conditions for strength development during the curing period. The inclusion of FA in the GPC mix resulted in improved strength development, as evidenced by the significant increase in split tensile strength for the RFG5 mix.

The interaction between FA and the other materials, such as BR and GGBS, likely contributed to enhanced bonding and interlocking of the geopolymer matrix, leading to improved tensile strength (Tammam et al. 2021). Overall, the results show the influence of material composition and curing time on the split tensile strength of geopolymer concrete. The data demonstrate that increasing the curing duration promotes strength development, and incorporating FA in the mix can significantly enhance the splitting resistance of GPC.

3.5 Relation Between Mechanical Properties

Understanding the mechanical properties and behavior of geopolymer concrete requires a comprehensive analysis of the correlation between compressive strength, flexural strength, and split tensile strength. This innovative construction material's 28-day strength properties are particularly important to examine. To predict the flexural and split tensile strength of geopolymer concrete, it is crucial to investigate the relationship between these strengths. Establishing such a correlation enables the estimation of flexural and split tensile strengths based on the known compressive strength. The graphical representations of these findings can be observed in Figs. 8 and 9. From Figs. 8 and 9, the flexural and split tensile strength can be obtained from the known compressive strength.

3.6 Durability Test

3.6.1 RCPT Test

The variation of charge transmitted as measured using a geopolymer specimen is shown in Fig. 10. The provided results describe the variation of charge passed, measured using a test called the rapid chloride penetration test (RCPT), with different geopolymer specimens labeled as RFG1, RFG2, RFG3, RFG4, RFG5, RFG6, and RFG7. The results are reported for three different durations: 30, 60, and 90 days. According to the given results, the electrical conductivity (charge passed) values for each of the geopolymer specimens

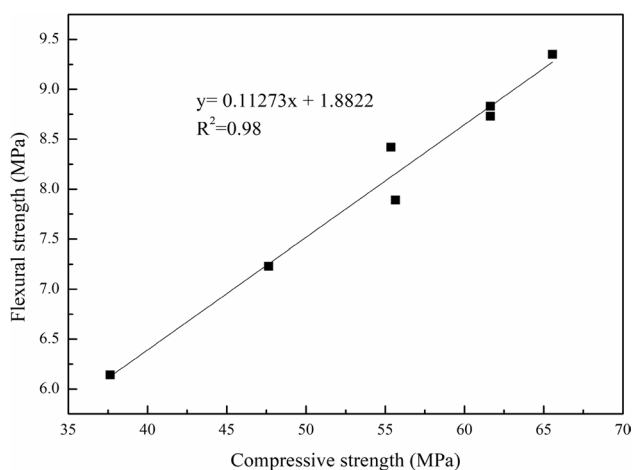


Fig. 8 Correlation of compressive strength with flexural strength

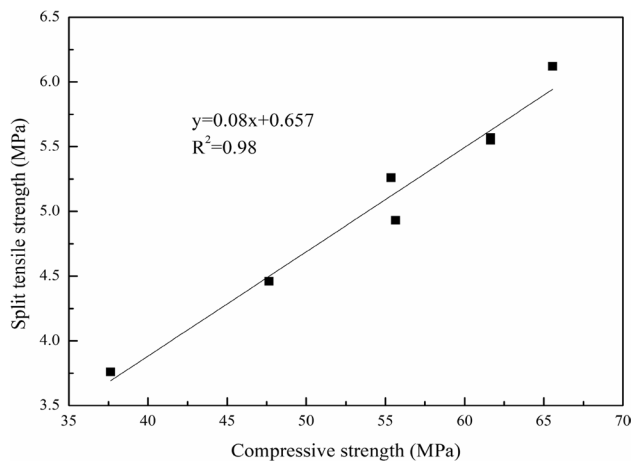


Fig. 9 Correlation of compressive strength with split tensile strength

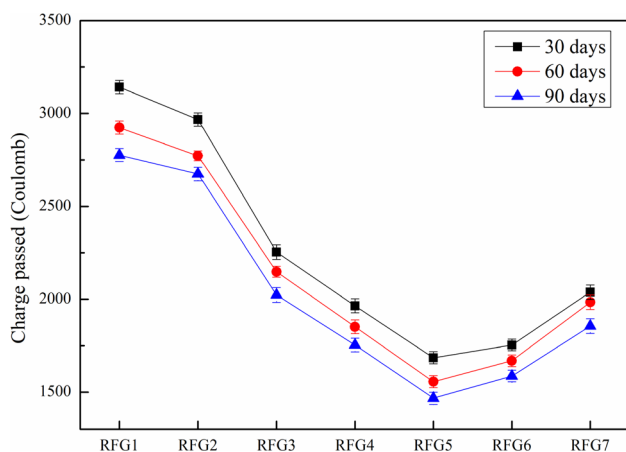


Fig. 10 RCPT of GPC at different duration

vary over the three time periods. For instance, at 30 days, the electrical conductivity values for RFG1, RFG2, RFG3, RFG4, RFG5, RFG6, and RFG7 are 3142, 2967, 2254, 1965, 1685, 1754, and 2038 C, respectively. These values decrease at 60 days, with electrical conductivity values of 2924, 2772, 2148, 1852, 1556, 1669, and 1984 C for the same mix. Similarly, at 90 days, the values further decrease to 2776, 2674, 2023, 1754, 1467, 1587, and 1856 C, respectively. The trend depicted in the results suggests that as the geopolymer specimens undergo longer curing periods, their electrical conductivity, and consequently their permeability to chloride ions, decreases. This trend is generally desirable as it indicates an improvement in the material's durability and ability to withstand chloride-induced corrosion.

From the provided results, it is observed that the electrical conductivity (charge passed) decreases as the strength of the geopolymer concrete increases. The higher strength of the geopolymer material corresponds to lower values of charge passed. This suggests that geopolymer specimens with higher strength exhibit lower electrical conductivity and, therefore, better durability against chloride ion penetration. The relationship between concrete strength and resistance to chloride ion penetration is well-known in the field of construction materials. High-strength concrete typically has a lower porosity, which restricts the movement of chloride ions through the material (Badkul et al. 2021; Chen et al. 2021; Gupta and Siddique 2020). As a result, less electrical charge passes through the specimen during the RCPT, indicating a higher resistance to chloride ion penetration and improved durability. The presented results indicate that the geopolymer specimens with higher strength (RFG5) have lower charge passed values, suggesting better durability against chloride ion penetration. On the other hand, geopolymer specimens with lower strength (RFG1) exhibit higher charge passed values, indicating reduced durability.

3.6.2 Water Absorption and Porosity Test

Figure 11 displays the water absorption and porosity characteristics of the geopolymer concrete following a 28-day period of curing. Both porosity and water absorption exhibit a similar trend. The porosity values for different formulations, labeled as RFG1, RFG2, RFG3, RFG4, RFG5, RFG6, and RFG7, are recorded as 13.13, 11.32, 10.54, 8.76%, 7.11, 8.28, and 9.16%, respectively. Similarly, the water absorption values for the same formulations are documented as 5.13, 4.45, 4.17, 3.18, 2.52, 3.18, and 3.67%, respectively. Notably, the porosity and water absorption display their minimum values when 25% of bauxite residue is replaced with fly ash at a constant 10% GGBS content. Analyzing the data presented in the figure, it is apparent that the substitution of bauxite residue with fly ash at a fixed GGBS content of 10% results in a decrease in both porosity and water absorption in

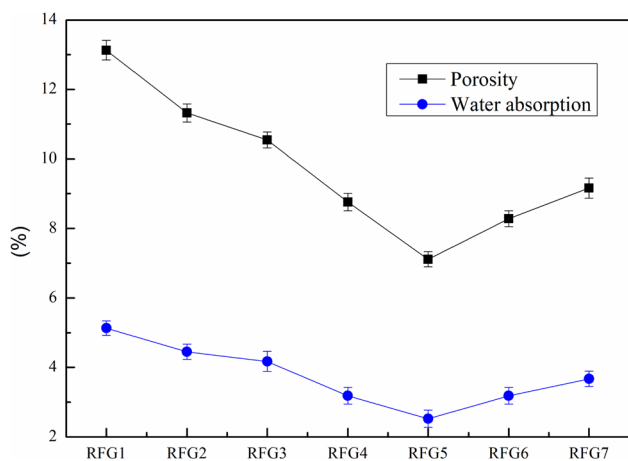


Fig. 11 Porosity and water absorption of the GPC

the geopolymer concrete. The lowest porosity value among the investigated formulations is achieved when 25% of bauxite residue is replaced with fly ash. This implies that this specific combination of materials leads to a denser concrete with fewer interconnected voids, consequently reducing the permeability of water into the material (Durak et al. 2021; Pouhet and Cyr 2016; Zhang et al. 2018).

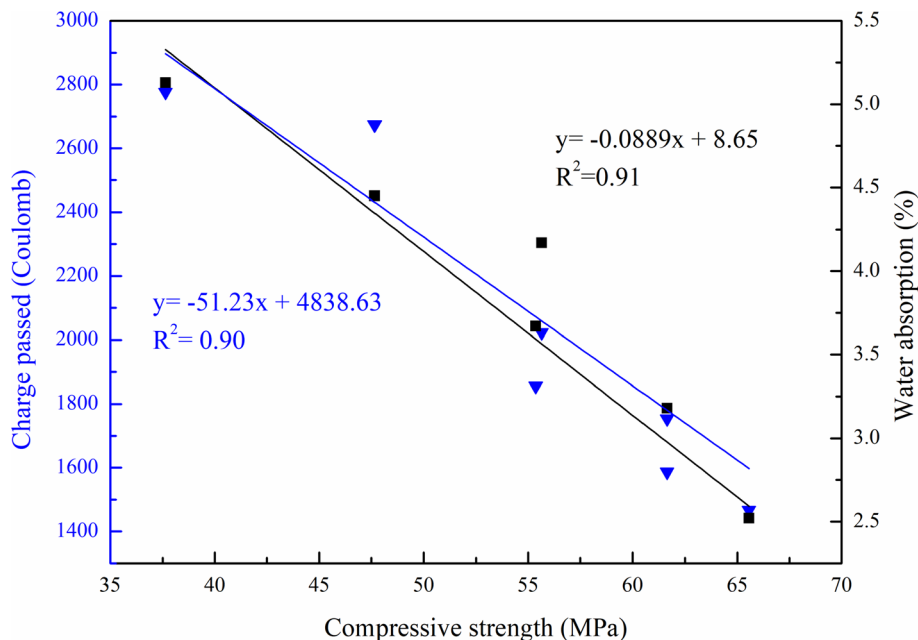
Lower water absorption indicates that the concrete is less susceptible to water ingress and, consequently, provides improved durability. The observed trend can be attributed to the properties of fly ash and its influence on the geopolymerization process. When fly ash used as a partial replacement for bauxite residue in geopolymer concrete, it reacts with alkaline activator, to form a geopolymer matrix. This matrix fills the voids in the concrete and contributes to the

densification of the material (Durak et al. 2021). The reaction between fly ash and the alkaline activators generates additional binding compounds, resulting in reduced porosity and water absorption. Furthermore, the constant GGBS content of 10% in all formulations suggests that GGBS plays a secondary role in affecting the porosity and water absorption characteristics. Additionally, excessive fly ash can lead to more porous structure formed increased water absorption. The higher water absorption can negatively affect the overall strength development, as it show the increased porosity and reduced density of the hardened material (Zhang et al. 2020b).

3.7 Relationship Between Compressive Strength and Durability Properties

Figure 12 illustrates the correlation between the strength and durability properties of geopolymer concrete. The data presented in the figure were collected at various time intervals: the compressive strength was measured after 28 days, while the RCPT and water absorption were evaluated after 90 days and 28 days, respectively. Upon analyzing the figure, it becomes evident that there is an inverse relationship between the strength of the concrete and both RCPT and water absorption. In other words, as the compressive strength increases, the RCPT and water absorption decrease. This finding suggests that higher strength levels are indicative of improved durability properties in geopolymer concrete. To further quantify the strength-durability relationship, statistical analysis was performed using the coefficient of determination, denoted as R^2 . The R^2 value is a measure of how closely the data points fit the regression line. In this

Fig. 12 Relation between strength vs durability properties



case, the R^2 value for the relationship between compressive strength and RCPT is determined to be 0.90, while the R^2 value for the relationship between compressive strength and water absorption is 0.91. These R^2 values, both above 0.9, indicate a strong correlation between compressive strength and durability properties. A high R^2 value suggests that approximately 90% of the variation observed in the RCPT and water absorption can be explained by changes in compressive strength. Therefore, the compressive strength of geopolymer concrete is a reliable indicator of its resistance to chloride penetration and water absorption. The significance of these findings lies in the implications for practical applications. Geopolymer concrete with higher compressive strength values can be expected to exhibit reduced RCPT and water absorption properties. This implies that structures constructed using geopolymer concrete with greater strength will be more durable and resistant to the ingress of chloride ions and water.

3.8 Effect of Salinity, Acid and Sulfate Environment on the Geopolymer Concrete

3.8.1 Mass Loss

The mass loss of hardened GPC specimens under the influence of chloride, acid, and sulfate attack are depicted in Fig. 13. The incorporation of Fly Ash (FA) in all the GPC mixes resulted in a decrease in mass loss. The specific GPC mixes, namely RFG1, RFG2, RFG3, RFG4, RFG5, RFG6, and RFG7, were subjected to chloride attack, and their respective mass losses were found to be 6.15, 5.83, 5.25, 4.94, 3.92, 4.13, and 4.32%. This indicates that the inclusion of FA led to reduced mass loss in all the mixes. A similar trend was detected when the GPC specimens were subjected to acid and sulfate attack. The mass loss in the acid and

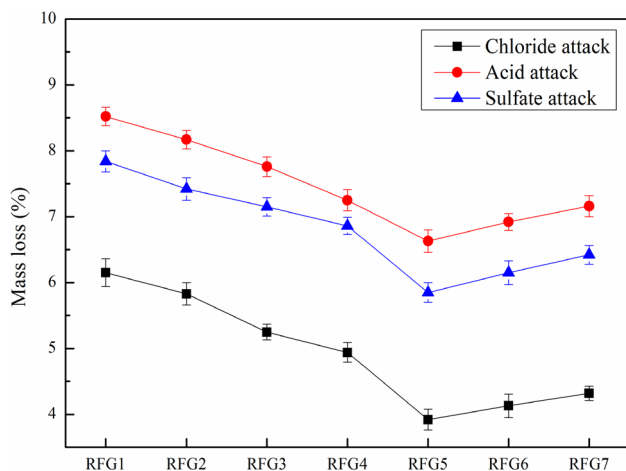


Fig. 13 Mass loss in different environmental condition

sulfate-rich environments was also lower for all the considered mixes when FA was incorporated. However, it was noted that the RFG5 mix performed exceptionally well in all three environments: chloride, acid, and sulfate. In comparison to the other mixes, RFG5 suffered less than 9% mass loss in acid attack, whereas specimens exposed to chloride ions experienced a noteworthy loss of about 6% and for sulfate around 8%. It should be noted that acid attacks involve both physical and chemical degradation mechanisms. Therefore, the GPC sample exposed to acidic environment exhibited a higher mass loss compared to those exposed to chloride and sulfate solutions. Based on these findings, it can be concluded that the RFG5 mix of GPC shows promising performance in aggressive environments containing chloride and sulfate environment.

3.8.2 Strength Loss

The results are presented in Fig. 14, which shows the loss in strength of the GPC specimens when exposed to sulphate, acid, and chloride attack. From the figure, it can be observed that GPC exhibits better resistance to chloride environments compared to acid and sulfate solutions. The strength loss percentages for different GPC mixes for specimens RFG1, RFG2, RFG3, RFG4, RFG5, RFG6, and RFG7, in sulphate, acid, and chloride attack. The strength losses for these mixes range from 8.27 to 14.26%, 11.56 to 17.45% and 10.74 to 16.24% in chloride, acid and sulphate solution respectively, indicating that the GPC mixes have suffered some reduction in strength when exposed to aggressive ions. Furthermore, the passage mentions that the percentage loss in strength of the GPC mixes is higher than the loss in mass for the same mixes. This suggests that the deterioration of compressive strength is more significant than the loss of material mass in GPC RFG5 specimens subjected to aggressive ions.

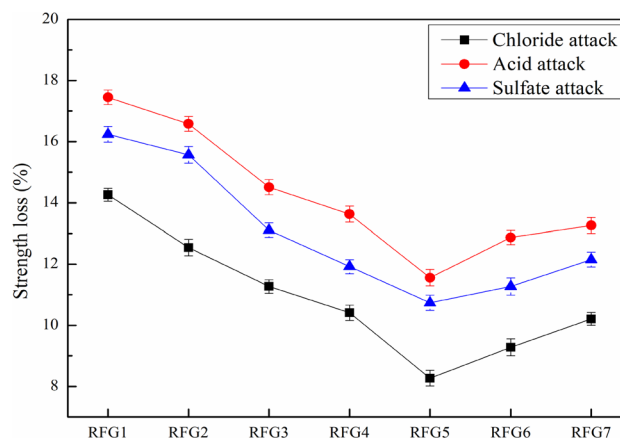


Fig. 14 Strength loss in different environmental conditions

3.9 Microcharacterisation of the Geopolymer Concrete

Figures 15, 16, 17, 18 are energy dispersion spectroscopy (EDS) images that depict the microstructure of samples, RFG1, RFG3, RFG5 and RFG7. The images reveal distinct differences in morphology between the specimens, indicating the influence of fly ash (FA) addition to BR and GGBS in the specimens. In Fig. 15, the micrograph of RFG1, unreacted particle units are clearly visible in a round shape. This suggests that the reaction between the FA, BR, and GGBS may not have been complete, leaving behind some unreacted particles. Additionally, small gel formations can be observed within the RFG3 specimen (Fig. 16). These gel formations may indicate the presence of partially reacted materials or the formation of secondary reaction products. In contrast,

Fig. 17 shows the EDS micrograph of RFG5. In this image, glare flocculent crystals are identified as C-A-S-H (calcium aluminosilicate hydrate) and N-A-S-H (sodium aluminosilicate hydrate) gels (Pratap et al. 2023b). The presence of these gels recommends that the replacement of FA to BR and GGBS has contributed to the formation of geopolymer gels (Tammam et al. 2021). Fly ash is known to contain significant amounts of Al^{3+} and Si^{4+} ions, which are essential components for the formation of geopolymer gels (Badkul et al. 2021). The formation of the gel in RFG5 may crucial to the increment of the strength of the specimen.

Energy dispersion X-ray (EDX) graphs that provide information about the elemental composition of samples RFG1, RFG3, RFG5 and RFG7. In Fig. 17, the EDX graph shows that RFG5 has silicon (Si), aluminum (Al), and calcium (Ca) contents. The presence of these elements in different

Fig. 15 EDS micrograph of RFG1 specimen

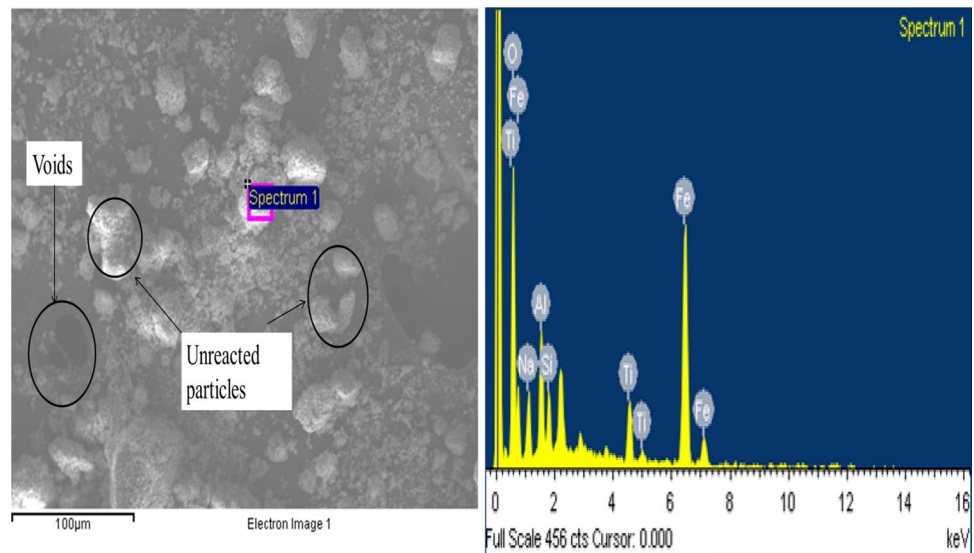


Fig. 16 EDS micrograph of RFG3 specimen

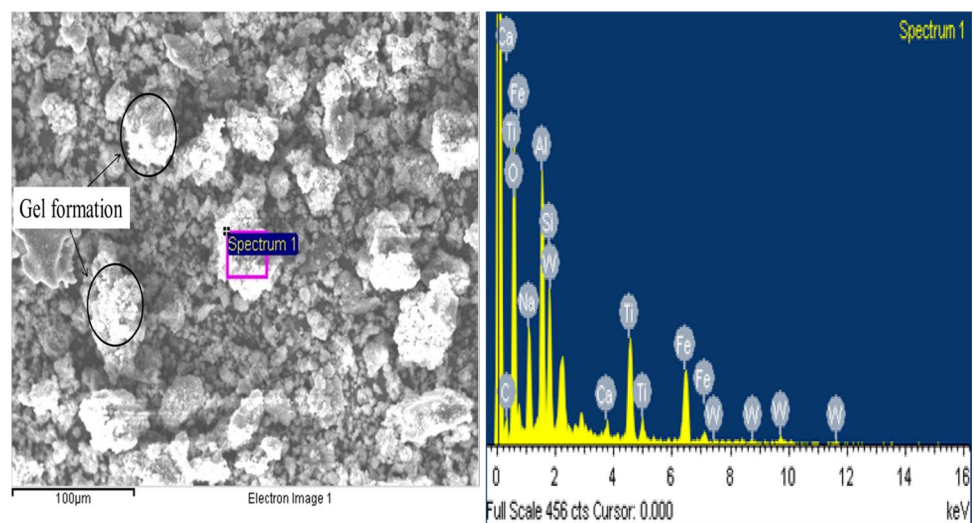


Fig. 17 EDS micrograph of RFG5 specimen

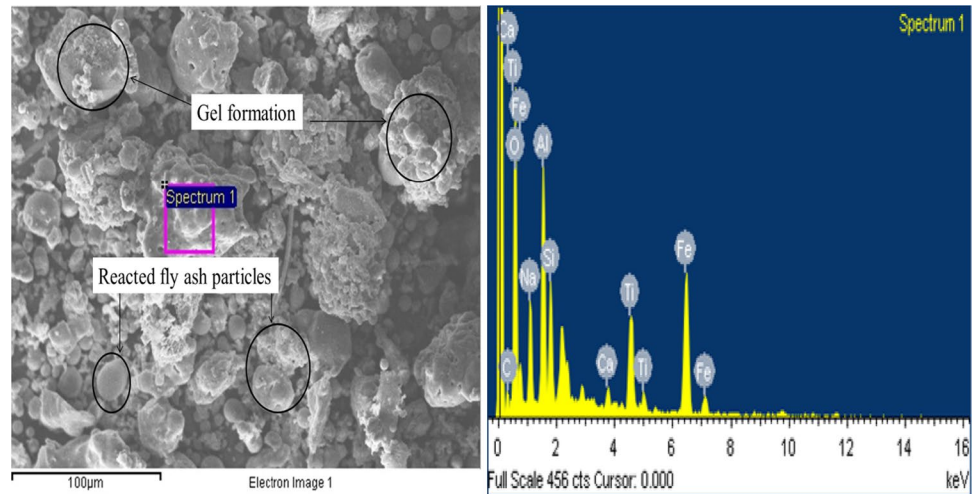
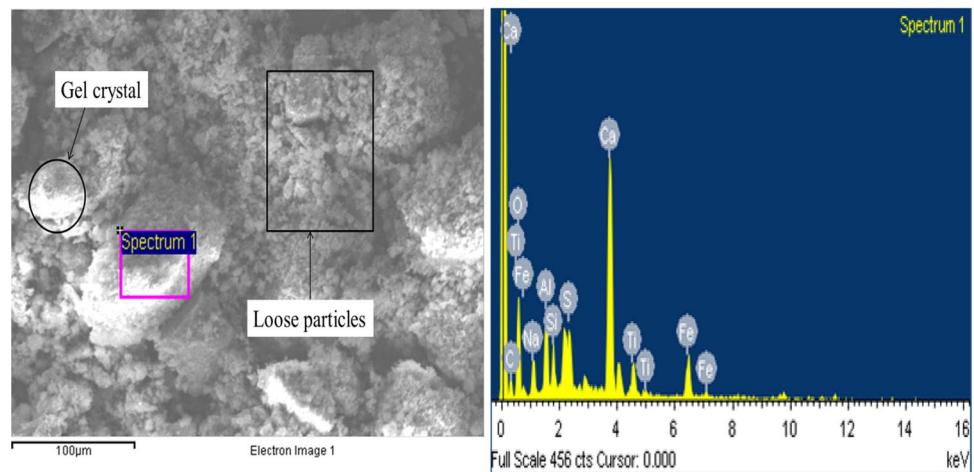


Fig. 18 EDS micrograph of RFG7 specimen



quantities suggests that they played a precarious role in the creation of gels in RFG5 (Xu and Shi 2018). Notably, there is an increase of iron (Fe) element in RFG1 (Fig. 15). This high content of Fe can have significant implications for the properties of the GPC. Furthermore, the presence of excess iron in RFG1 can also have detrimental effects. In the process of geopolymerization, iron elements do not actively participate in the hydration reaction to yield C-A-S-H/N-A-S-H gels (Badkul et al. 2021). Instead, they remain unreacted and can potentially weaken the overall structure of the geopolymer concrete. The high content of Fe seen in Fig. 15 indicates that RFG1 may have suffered from reduced strength due to the presence of elements. In contrast, Fig. 17 represents the EDX graph for RFG5. In this case, the silicon, calcium, and aluminum contents are considerably higher compared to RFG1. The increased presence of these elements in RFG5 is beneficial for the creation of C-A-S-H/N-A-S-H gels, which are essential in achieving higher strength in geopolymer concrete (Reddy et al. 2018). Therefore, the

higher Si, Ca, and Al contents observed in Fig. 17 suggest that RFG5 is more likely to exhibit increased strength compared to others specimens. It can be clearly observed that as the percentage of the fly ash increased then the loose particles can be seen in Fig. 18 (RFG7), that causes the strength loss of the specimen.

3.10 XRD Analysis

Figure 19 displays the outcomes of XRD tests on different mixes of geopolymer concrete. The degree of amorphousness and crystallization were considerably changed by geopolymerization, according to the identical XRD patterns for different mixes. The majority of the geopolymer was made up of amorphous aluminosilicate products, with only very small amounts of crystals, namely calcite and quartz from fly ash (Pratap et al. 2023c). Geopolymer's compressive strength rose as the amount of crystalline gels grew. The primary difference in the XRD patterns of the two materials

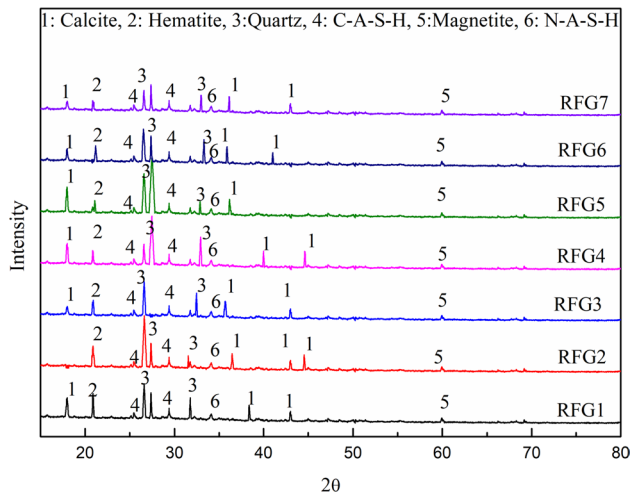


Fig. 19 XRD pattern of the different composite mixes

was the displacement of the amorphous quartz peak, which went from being around 25° to 30° for the geopolymer. This demonstrated the very chaotic nature of the silicate gel formation in geopolymer (Ojha and Aggarwal 2023). Another interesting small peak was between 28 degrees, where the graphs of the geopolymers show the formation of the C-A-S-H gels. The production of geopolymer gel may be the cause of the strength increment (Pratap et al. 2023a). Numerous huge and sharp peaks, which are associated with the mineral phases quartz and calcite, as well as medium to tiny peaks between 35 to 45 degree that are mostly related to calcite that help in the formation N-A-S-H gel at 35 degree after reaction with alkali solutions. Additionally, medium to tiny peaks between 2 of $25\text{--}50^\circ$ may be seen, suggesting the potential production of weakly crystalline C-A-S-H gel phases. In general, the existence of the minerals calcite, hematite, quartz and magnetite establishes the fact that the C-A-S-H and N-A-S-H gel structures were formed.

3.11 Leaching Analysis

While geopolymer concrete offers numerous advantages, its durability and mechanical properties must be thoroughly understood. One essential aspect of this understanding is the leaching characterization of geopolymer concrete. Leaching refers to the process by which soluble toxic components in a GPC are dissolved and transported away by water. In the context of GPC, leaching is a concern because it can potentially release harmful substances into the surrounding environment and impact water quality (Mishra et al. 2019). Therefore, it is crucial to characterize the leaching behavior of geopolymer concrete to ensure its environmental safety. One of the primary concerns regarding leaching in geopolymer concrete is the release of heavy metals and other

Table 3 leaching characterisation of raw and geopolymer concrete

Elements	Concentration (mg/L)				USEPA (TCLP) hazardous waste limit
	BR	FA	GGBS	RFG5	
As	0.02	2.04	1.04	Not found	5.0
Cr	0.32	3.65	2.72	0.001	5.0
Co	0.04	1.17	1.06	0.002	–
Cd	0.02	4.18	0.48	0.001	1.0
Pb	0.40	0.67	0.28	Not found	5.0
Ni	0.01	2.08	3.15	Not found	–
Hg	0.002	0.08	0.004	Not found	0.2
Zn	1.07	3.08	4.96	0.51	–
Cu	0.51	2.82	4.75	0.08	–
pH	10.12	8.73	10.26	7.42	6.5–8.5

potentially toxic elements (Mishra et al. 2020). The concentration of these elements must be kept below regulatory limits to ensure the concrete's safety and environmental compliance. Studies have shown that the leaching behavior of heavy metals in geopolymer concrete is typically lower compared to raw materials (Table 3). The concentration of the heavy metals in geopolymer concrete is reduced due to the solidification of the geopolymer gels (Pratap et al. 2023a). The developed gels help in the reduction of the heavy metals and pH. It can be clearly seen from the Table 3 that the reduced concentration of the heavy metals and pH is under the prescribed limit (EPA 1996). Hence, the developed geopolymer concrete is eco-friendly.

4 Applications and Recommendations

Geopolymer technology has emerged as a promising alternative to traditional cement-based materials in construction due to its advantageous mechanical and durability properties. In the context of rigid pavement, geopolymer concrete offers numerous benefits, including reduced carbon emissions, improved long-term performance, and increased resistance to environmental factors. This study provide a comprehensive review of the application of geopolymer in rigid pavement, specifically focusing on its mechanical and durability properties. According to IRC codes, the minimum compressive strength requirements for rigid pavement are well within the reach of geopolymer concrete (IRC 58 2011 2011). In this study have shown that geopolymer mixes can achieve compressive strengths exceeding 40 MPa, making them suitable for heavy traffic loads and industrial applications. Geopolymer concrete exhibits excellent resistance to acidic and alkaline environments, making it highly durable under various exposure conditions. This resistance is

especially critical in industrial areas where chemical spillage is common. The IRC guidelines emphasize the need for durable pavements to minimize maintenance and repair costs over the life of the infrastructure. The application of geopolymer in rigid pavement based on the mechanical and durability properties as per the IRC 58 (2011) shows promising results (IRC 58 2011 2011). Geopolymer concrete outperforms in terms of compressive strength, flexural strength, and meeting or exceeding IRC requirements for these properties. Moreover, geopolymer concrete's superior durability, including resistance to acids, alkalis, and chloride, makes it an excellent choice for long-lasting and sustainable infrastructure. Adopting geopolymer technology in rigid pavements can lead to reduced carbon emissions, extended pavement service life, and lower maintenance costs. However, it's essential to continue research and development efforts to optimize geopolymer mixes and ensure consistent performance under different site conditions. With ongoing advancements and growing awareness of sustainable construction practices, geopolymer concrete is poised to play a significant role in the future of rigid pavement construction.

5 Conclusions

This section highlights the conclusions of GPC which are developed by utilizing waste materials BR, FA, and GGBS.

- The compressive strength values of the GPC increase over time, with higher values observed at 28 days compared to the 3-day results. The flexural strength also improves at 28 days, with the highest value achieved when 25% of bauxite residue is replaced with 25% fly ash and 10% ground granulated blast furnace slag (RFG5).
- After 28 days, the split tensile strength of the geopolymer concrete also increases, with the highest value obtained when 25% of BR is replaced with FA and 10% with GGBS (RFG5 sample). The electrical conductivity of the geopolymer concrete decreases as its strength increases. Furthermore, the porosity and water absorption values decrease when 25% of BR is replaced with FA and 10% with GGBS.
- The RFG5 specimen resulted minimum mass and strength loss in acid, chloride and sulfate environment, which has the maximum strength, was obtained.
- It can be observed from the EDS micrograph the presence of bright, fluffy crystals known as C-A-S-H and N-A-S-H gels. These gels indicate that the addition of FA to BR and GGBS has contributed to the creation of geopolymer gels. Fly ash is recognized for containing significant amounts of Al^{3+} and Si^{4+} ions, which are crucial components for the formation of geopolymer gels.

The development of the gel in RFG5 may enhance the strength of the specimen.

- Overall, the results demonstrate that the geopolymerization process and the development of the binding matrix contribute to significant strength gains in the geopolymer concrete, and specific material compositions can influence the properties of the concrete, such as strength, electrical conductivity, porosity, and water absorption.
- It can be concluded that geopolymer concrete exhibits lower leaching of heavy metals when compared to raw materials. The solidification of geopolymer gels is responsible for reducing the concentration of heavy metals in geopolymer concrete.

Author's Contribution BP: Methodology, Investigation, Writing—original draft. PK: Review and editing. SM: Writing—review, editing and Supervision. BHR: Conceptualization, Methodology, editing and Supervision.

Funding No funding to declare.

Data Availability Data will be made available on request from the corresponding author.

Declarations

Conflict of interest The authors declare that there is no conflict of interest regarding the publication of this paper.

References

- Adamu M, Ibrahim, S, Yasser H, Hani EI (2022) Evaluation of the mechanical performance of concrete containing calcium carbide residue and nano silica using response surface methodology. *Environ Sci Pollut Res*. Springer, Berlin . <https://doi.org/10.1007/s11356-022-20546-x>.
- Alam S, Das SK, Rao BH (2019) Strength and durability characteristic of alkali activated GGBS stabilized red mud as geo-material. *Constr Build Mater* 211:932–942. <https://doi.org/10.1016/j.conbuilmat.2019.03.261>
- Apithanyasai S, Supakata N, Papong S (2020) The potential of industrial waste: using foundry sand with fly ash and electric arc furnace slag for geopolymer brick production. *Heliyon* 6(3):e03697. <https://doi.org/10.1016/j.heliyon.2020.e03697>
- ASTM C1202 (2012) Standard test method for electrical indication of concrete's ability to resist chloride ion penetration. *Am Soc Test Mater (C)*:1–8. <https://doi.org/10.1520/C1202-12.2>
- ASTM C143/C143M—10 (2014). *Astm C143. i* (Reapproved), pp 1–4. <https://doi.org/10.1520/C0143>
- ASTM C642 (2013) Standard test method for density, absorption, and voids in hardened concrete. *ASTM International, United States*. *Annu B ASTM Stand*, pp 1–3
- Badkul A, Paswan R, Singh SK, Tegar JP (2021) A comprehensive study on the performance of alkali activated fly ash/GGBFS geopolymer concrete pavement ash/GGBFS geopolymer concrete pavement. (May). <https://doi.org/10.1080/14680629.2021.1926311>.

- Bellum RR, Muniraj K, Indukuri CSR, Madduru SRC (2020a) Investigation on performance enhancement of fly ash-GGBFS based graphene geopolymer concrete. *J Build Eng* 32:101659. <https://doi.org/10.1016/j.jobe.2020.101659>
- Bellum RR, Muniraj K, Madduru SRC (2020b) Characteristic evaluation of geopolymer concrete for the development of road network: sustainable infrastructure. *Innov Infrastruct Solut* 5(3):244. <https://doi.org/10.1007/s41062-020-00344-5>
- Chen K, Wu D, Xia L, Cai Q, Zhang Z (2021) Geopolymer concrete durability subjected to aggressive environments—a review of influence factors and comparison with ordinary Portland cement. *Constr Build Mater* 279:122496. <https://doi.org/10.1016/j.conbuildmat.2021.122496>
- Chen S, Yuan H (2022) Characterization and optimization of eco-friendly cementitious materials based on titanium gypsum, fly ash, and calcium carbide residue. *Constr Build Mater* 349:128635. <https://doi.org/10.1016/j.conbuildmat.2022.128635>
- Deb PS, Nath P, Sarker PK (2014) The effects of ground granulated blast-furnace slag blending with fly ash and activator content on the workability and strength properties of geopolymer concrete cured at ambient temperature. *Mater Des* 62:32–39. <https://doi.org/10.1016/j.matdes.2014.05.001>
- Durak U, İlkentapar S, Karahan O, Uzal B, Atiş CD (2021) A new parameter influencing the reaction kinetics and properties of fly ash based geopolymers: a pre-rest period before heat curing. *J Build Eng* 35:102023. <https://doi.org/10.1016/j.jobe.2020.102023>
- EPA (1996) U.S. EPA. 1996. 'Method 3050B: acid digestion of sediments, sludges, and soils,' Revision 2. Washington, DC." EPA, 18 (7):723. https://doi.org/10.18907/jjsre.18.7_723_2
- Fareed Ahmed M, Fadhil Nuruddin M, Shafiq N (2011) Compressive strength and workability characteristics of low-calcium fly ash-based self-compacting geopolymer concrete. *World Acad Sci Eng Technol* 74(February):8–14. <https://doi.org/10.5281/zenodo.1330481>
- Fernando S, Gunasekara C, Law DW, Nasvi MCM, Setunge S, Disanayake R (2023) Assessment of long term durability properties of blended fly ash-Rice husk ash alkali activated concrete. *Constr Build Mater* 369:130449. <https://doi.org/10.1016/j.conbuildmat.2023.130449>
- Gupta N, Siddique R (2020) Durability characteristics of self-compacting concrete made with copper slag. *Constr Build Mater* 247:118580. <https://doi.org/10.1016/j.conbuildmat.2020.118580>
- Hoang MD, Do QM, Le VQ (2020) Effect of curing regime on properties of red mud based alkali activated materials. *Constr Build Mater* 259:119779. <https://doi.org/10.1016/j.conbuildmat.2020.119779>
- Iqbal HW, Hamcumpai K, Nuaklong P, Jongvivatsakul P, Likitlersuang S, Chintanapakdee C, Wijeyewickrema AC (2023) Effect of graphene nanoplatelets on engineering properties of fly ash-based geopolymer concrete containing crumb rubber and its optimization using response surface methodology. *J. Build. Eng.* 75:107024. <https://doi.org/10.1016/j.jobe.2023.107024>
- IRC 58 2011 (2011) Standard specifications and code of practice for construction of concrete roads. *Irc* 15(2011):1–89
- IS:10086 (2004) Indian Standard Reaffirmed 2004 Reaffirmed 2008 SPECIFICATION FOR MOULDS FOR USE IN TESTS OF CEMENT AND CONCRETE
- Jatoliya A, Saha S, Pratap B, Mondal S (2023) Assessment of bauxite residue stabilized with lime and graphene oxide as a geomaterial for road applications. *Soils Rocks* 46(1):1–13
- John SK, Nadir Y, Girija K (2021) Effect of source materials, additives on the mechanical properties and durability of fly ash and fly ash-slag geopolymer mortar: a review. *Constr Build Mater* 280:122443. <https://doi.org/10.1016/j.conbuildmat.2021.122443>
- Koshy N, Dondrob K, Hu L, Wen Q, Meegoda JN (2019) Synthesis and characterization of geopolymers derived from coal gangue, fly ash and red mud. *Constr Build Mater* 206:287–296. <https://doi.org/10.1016/j.conbuildmat.2019.02.076>
- Kumar A, Kumar S (2013) Development of paving blocks from synergistic use of red mud and fly ash using geopolymerization. *Constr Build Mater* 38:865–871. <https://doi.org/10.1016/j.conbuildmat.2012.09.013>
- Kuri JC, Sarker PK, Uddin F, Shaikh A (2021) Sulphuric acid resistance of ground ferronickel slag blended fly ash geopolymer mortar. *Constr Build Mater* 313:125505. <https://doi.org/10.1016/j.conbuildmat.2021.125505>
- Li Y, Liu X, Li Z, Ren Y, Wang Y, Zhang W (2021) Preparation, characterization and application of red mud, fly ash and desulfurized gypsum based eco-friendly road base materials. *J Clean Prod* 284:124777. <https://doi.org/10.1016/j.jclepro.2020.124777>
- Li Z, Zhang J, Li S, Gao Y, Liu C, Qi Y (2020) Effect of different gypsums on the workability and mechanical properties of red mud-slag based grouting materials. *J Clean Prod* 245:118759. <https://doi.org/10.1016/j.jclepro.2019.118759>
- Lian C, Wang Y, Liu S, Hao H, Hao Y (2023) Experimental study on dynamic mechanical properties of fly ash and slag based alkali-activated concrete. *Constr Build Mater* 364:129912. <https://doi.org/10.1016/j.conbuildmat.2022.129912>
- Liang X, Ji Y (2021) Mechanical properties and permeability of red mud-blast furnace slag-based geopolymer concrete. *SN Appl Sci* 3(1):1–10. <https://doi.org/10.1007/s42452-020-03985-4>
- Liu MYJ, Alengaram UJ, Santhanam M, Jumaat MZ, Mo KH (2016) Microstructural investigations of palm oil fuel ash and fly ash based binders in lightweight aggregate foamed geopolymer concrete. *Constr Build Mater* 120:112–122. <https://doi.org/10.1016/j.conbuildmat.2016.05.076>
- Ma F, Chen L, Lin Z, Liu Z, Zhang W, Guo R (2022) Microstructure and key properties of phosphogypsum-red mud-slag composite cementitious materials. *Materials (basel)* 15(17):1–18. <https://doi.org/10.3390/ma15176096>
- Meesala CR, Verma NK, Kumar S (2020) Critical review on fly-ash based geopolymer concrete. *Struct Concr* 21(3):1013–1028. <https://doi.org/10.1002/suco.201900326>
- Meskini S, Remmal T, Ejjaouani H, Samdi A (2022) Formulation and optimization of a phosphogypsum—fly ash—lime composite for road construction : a statistical mixture design approach. *Constr Build Mater* 315:125786. <https://doi.org/10.1016/j.conbuildmat.2021.125786>
- Mishra MC, Babu KS, Reddy NG, Dey PP, Rao BH (2019) Performance of lime stabilization on extremely alkaline red mud waste under acidic environment. *J Hazard Toxic Radioactive Waste* 23(4):1–14. [https://doi.org/10.1061/\(ASCE\)JHZ.2153-5515.0000448](https://doi.org/10.1061/(ASCE)JHZ.2153-5515.0000448)
- Mishra MC, Reddy NG, Rao BH (2020) Potential of citric acid for treatment of extremely alkaline bauxite residue: effect on geotechnical and geoenvironmental properties. *J Hazard Toxic Radioactive Waste* 24(4):04020047. [https://doi.org/10.1061/\(asce\)jhz.2153-5515.0000541](https://doi.org/10.1061/(asce)jhz.2153-5515.0000541)
- Muraleedharan M, Nadir Y (2021a) Factors affecting the mechanical properties and microstructure of geopolymers from red mud and granite waste powder: a review. *Ceram Int*. <https://doi.org/10.1016/j.ceramint.2021.02.009>
- Muraleedharan M, Nadir Y (2021b) Factors affecting the mechanical properties and microstructure of geopolymers from red mud and granite waste powder: a review. *Ceram Int* 47(10PA):13257–13279. <https://doi.org/10.1016/j.ceramint.2021.02.009>
- Naenudon S, Wongs A, Ekprasert J, Sata V, Chindaprasirt P (2023) Enhancing the properties of fly ash-based geopolymer concrete using recycled aggregate from waste ceramic electrical insulator.

- J. Build. Eng. 68:106132. <https://doi.org/10.1016/j.jobbe.2023.106132>
- Nath P, Sarker PK (2017) Flexural strength and elastic modulus of ambient-cured blended low-calcium fly ash geopolymer concrete. *Constr Build Mater* 130:22–31. <https://doi.org/10.1016/j.conbuildmat.2016.11.034>
- Ngarm P, Chindaprasirt P, Sata V (2015) Setting time, strength, and bond of high-calcium fly ash geopolymer concrete. *J Mater Civ Eng* 27(7):04014198. [https://doi.org/10.1061/\(asce\)mt.1943-5533.0001157](https://doi.org/10.1061/(asce)mt.1943-5533.0001157)
- Ojha A, Aggarwal P (2023) Durability performance of low calcium Flyash-Based geopolymer concrete. *Structures* 54:956–963. <https://doi.org/10.1016/j.istruc.2023.05.115>
- Özkılıç YO, Çelik Aİ, Tunç U, Karalar M, Deifalla A, Alomayri T, Althoey F (2023) The use of crushed recycled glass for alkali activated fly ash based geopolymer concrete and prediction of its capacity. *J Mater Res Technol* 24:8267–8281. <https://doi.org/10.1016/j.jmrt.2023.05.079>
- Pouhet R, Cyr M (2016) Formulation and performance of flash metakaolin geopolymer concretes. *Constr Build Mater* 120:150–160. <https://doi.org/10.1016/j.conbuildmat.2016.05.061>
- Pratap B, Mondal S, Hanumantha Rao B (2023a) Synthesis of alkali-activated mortar using phosphogypsum-neutralised bauxite residue. *Environ Geotech* 22:1–12. <https://doi.org/10.1680/jenge.22.00104>
- Pratap B, Mondal S, Hanumantha Rao B (2023b) Development of geopolymer concrete using fly ash and phosphogypsum as a pavement composite material. *Mater Today Proc* 6:207. <https://doi.org/10.1016/j.matpr.2023.06.207>
- Pratap B, Mondal S, Rao BH (2023c) Mechanical and durability analysis of geopolymer concrete incorporating bauxite residue, phosphogypsum, and ground granulated blast slag. *Asian J. Civ. Eng.* 23:777. <https://doi.org/10.1007/s42107-023-00777-0>
- Pratap B, Mondal S, Rao BH (2024) Mechanical and durability assessment of phosphogypsum- bauxite residue - fly ash-based alkali-activated concrete. *Constr Build Mater* 411:134670. <https://doi.org/10.1016/j.conbuildmat.2023.134670>
- Pratap B, Shubham K, Mondal S, Hanumantha B (2023d) Exploring the potential of neural network in assessing mechanical properties of geopolymer concrete incorporating fly ash and phosphogypsum in pavement applications. *Civ Eng Asian J.* <https://doi.org/10.1007/s42107-023-00735-w>
- Reddy MS, Dinakar P, Rao BH (2018) Mix design development of fly ash and ground granulated blast furnace slag based geopolymer concrete. *J Build Eng* 20:712–722. <https://doi.org/10.1016/j.jobbe.2018.09.010>
- Ren Z, Wang L, Wang H, Liu S, Liu M (2023) Solidification/stabilization of lead-contaminated soils by phosphogypsum slag-based cementitious materials. *Sci Total Environ* 857:159552. <https://doi.org/10.1016/j.scitotenv.2022.159552>
- Ryu GS, Lee YB, Koh KT, Chung YS (2013) The mechanical properties of fly ash-based geopolymer concrete with alkaline activators. *Constr Build Mater* 47:409–418. <https://doi.org/10.1016/j.conbuildmat.2013.05.069>
- Sahu A, Kumar S, Srivastava AKL, Pratap B (2024) Performance of recycled aggregate concrete using copper slag as fine aggregate. *J Build Eng* 82:108364. <https://doi.org/10.1016/j.jobbe.2023.108364>
- Sarath Chandra K, Krishnaiah S (2022) Strength and leaching characteristics of red mud (bauxite residue) as a geomaterial in synergy with fly ash and gypsum. *Transp Res Interdiscip Perspect* 13:100566. <https://doi.org/10.1016/j.trip.2022.100566>
- Shahmansouri AA, Nematzadeh M, Behnood A (2021) Mechanical properties of GGBFS-based geopolymer concrete incorporating natural zeolite and silica fume with an optimum design using response surface method. *J Build Eng* 36:102138. <https://doi.org/10.1016/j.jobbe.2020.102138>
- Shi X, Zhang C, Wang X, Zhang T, Wang Q (2022) Response surface methodology for multi-objective optimization of fly ash-GGBS based geopolymer mortar. *Constr Build Mater* 315:125644. <https://doi.org/10.1016/j.conbuildmat.2021.125644>
- Singh S, Aswath MU, Ranganath RV (2018) Effect of mechanical activation of red mud on the strength of geopolymer binder. *Constr Build Mater* 177:91–101. <https://doi.org/10.1016/j.conbuildmat.2018.05.096>
- Sudhir MR, Beulah M, Sasha Rai P, Gayathri G (2020) A microstructure exploration and compressive strength determination of red mud bricks prepared using industrial wastes. *Mater Today Proc.* <https://doi.org/10.1016/j.matpr.2020.07.171>
- Sun B, Sun Y, Ye G, De Schutter G (2022) A mix design methodology of slag and fly ash-based alkali-activated paste. *Cem Concr Compos* 126:104368. <https://doi.org/10.1016/j.cemconcomp.2021.104368>
- Tammam Y, Uysal M, Canpolat O (2021) Effects of alternative ecological fillers on the mechanical, durability, and microstructure of fly ash-based geopolymer mortar. *Eur J Environ Civ Eng* 19:1–24. <https://doi.org/10.1080/19648189.2021.1925157>
- Tanyildizi H, Yonar Y (2016) Mechanical properties of geopolymer concrete containing polyvinyl alcohol fiber exposed to high temperature. *Constr Build Mater* 126:381–387. <https://doi.org/10.1016/j.conbuildmat.2016.09.001>
- Toniolo N, Rincón A, Avadhut YS, Hartmann M, Bernardo E, Boccaccini AR (2018) Novel geopolymers incorporating red mud and waste glass cullet. *Mater Lett* 219:152–154. <https://doi.org/10.1016/j.matlet.2018.02.061>
- Vafaei M, Allahverdi A, Dong P, Bassim N, Mahinroosta M (2021) Resistance of red clay brick waste/phosphorus slag-based geopolymer mortar to acid solutions of mild concentration. *J Build Eng* 34:102066. <https://doi.org/10.1016/j.jobbe.2020.102066>
- Xie T, Ozbakkaloglu T (2015) Behavior of low-calcium fly and bottom ash-based geopolymer concrete cured at ambient temperature. *Ceram Int* 41(4):5945–5958. <https://doi.org/10.1016/j.ceramint.2015.01.031>
- Xu G, Shi X (2018) Characteristics and applications of fly ash as a sustainable construction material: A state-of-the-art review. *Resour Conserv Recycl* 136:95–109. <https://doi.org/10.1016/j.resconrec.2018.04.010>
- Yang Z, Mocadro R, Zhao M, Sisson RD, Tao M, Liang J (2019) Preparation of a geopolymer from red mud slurry and class F fly ash and its behavior at elevated temperatures. *Constr Build Mater* 221:308–317. <https://doi.org/10.1016/j.conbuildmat.2019.06.034>
- Yin S, Yan Z, Chen X, Wang L (2022) Effect of fly-ash as fine aggregate on the workability and mechanical properties of cemented paste backfill. *Case Stud Constr Mater* 16:e01039. <https://doi.org/10.1016/j.cscm.2022.e01039>
- Zakira U, Zheng K, Xie N, Birgisson B (2023) Development of high-strength geopolymers from red mud and blast furnace slag. *J Clean Prod* 383:135439. <https://doi.org/10.1016/j.jclepro.2022.135439>
- Zhang J, Li S, Li Z (2020a) Investigation the synergistic effects in ternary binder containing red mud, blast furnace slag, steel slag and flue gas desulfurization gypsum based on artificial neural networks. *J Clean Prod* 273:122972. <https://doi.org/10.1016/j.jclepro.2020.122972>
- Zhang J, Li S, Li Z, Liu C, Gao Y (2020b) Feasibility study of red mud for geopolymer preparation: effect of particle size fraction. *J Mater Cycles Waste Manag* 22(5):1328–1338. <https://doi.org/10.1007/s10163-020-01023-4>
- Zhang J, Yao Z, Wang K, Wang F, Jiang H, Liang M, Wei J, Airey G (2021) Sustainable utilization of bauxite residue (Red Mud) as a road material in pavements: a critical review. *Constr Build Mater* 270:121419. <https://doi.org/10.1016/j.conbuildmat.2020.121419>
- Zhang M, Zhao M, Zhang G, Sietins JM, Granados-Focil S, Pepi MS, Xu Y, Tao M (2018) Reaction kinetics of red mud-fly ash based geopolymers: Effects of curing temperature on chemical bonding,

porosity, and mechanical strength. *Cem Concr Compos* 93:175–185. <https://doi.org/10.1016/j.cemconcomp.2018.07.008>

Zhou W, Shi X, Lu X, Qi C, Luan B, Liu F (2020) The mechanical and microstructural properties of refuse mudstone-GGBS-red mud based geopolymer composites made with sand. *Constr Build Mater* 253:119193. <https://doi.org/10.1016/j.conbuildmat.2020.119193>

Springer Nature or its licensor (e.g. a society or other partner) holds exclusive rights to this article under a publishing agreement with the author(s) or other rightsholder(s); author self-archiving of the accepted manuscript version of this article is solely governed by the terms of such publishing agreement and applicable law.